



Seismic Demands on Steel Diaphragms for 3D Archetype Buildings with Concentric Braced Frames

H. Foroughi¹, G. Wei², S. Torabian³, M. R. Eatherton⁴, and B.W. Schafer⁵

¹ Graduate Research Assistant, Dept. of Civil Engineering, Johns Hopkins University, hforoug1@jhu.edu

² Graduate Research Assistant, Dept. of Civil Engineering, Virginia Tech, gwei1@vt.edu

³ Associate Research Scientist, Dept. of Civil Engineering, Johns Hopkins University, torabian@jhu.edu

⁴ Associate Professor, Dept. of Civil Engineering, Virginia Tech, meather@vt.edu

⁵ Professor, Dept. of Civil Engineering, Johns Hopkins University, schaffer@jhu.edu

ABSTRACT

The objective of this research is to explore the impact of the vertical bracing system on the seismic demands and response of floor diaphragms in steel buildings. A unique feature of the investigation is the creation of fully three-dimensional building models so that the interaction of the horizontal and vertical lateral force resisting systems can be explored. Most investigations on the seismic performance of building systems have focused on the performance of the vertical lateral force resisting system and have employed nonlinear, but two-dimensional, models. To ground the models in reality a one-story steel-framed archetype building is designed to current and proposed provisions. A steel concentric braced frames is considered for the vertical lateral force resisting system in the building. A series of nonlinear time history analyses on 3D building models developed in OpenSees are performed across the FEMA P695 earthquake suite at a variety of demand levels to assess the performance of the building with particular interest in the building diaphragm. This work is part of an initiative (www.steeli.org) to better understand the seismic performance of steel diaphragms in buildings and develop new innovations for steel deck diaphragms.

Keywords: steel deck, diaphragm, steel-framed archetype building, braced frame, diaphragm demands.

INTRODUCTION

The seismic performance of buildings depends on both the vertical lateral force resisting system (LFRS), such as braced frames, and the horizontal LFRS, such as the roof or floor diaphragm. Conventional seismic design of buildings assumes that the vertical LFRS is the only source of inelastic actions and hysteretic energy dissipation in the structure. However, it has been shown that diaphragms designed using traditional design procedures may be subject to inelasticity even during design level earthquakes [1], and in the extreme may experience collapse such as happened for several concrete parking garages with precast concrete diaphragms during the 1994 Northridge earthquake [2]. The role of the diaphragm in energy dissipation may be particularly pronounced for single-story structures when the story stiffness is far greater than the in-plane diaphragm stiffness – a condition that can happen in steel buildings with braced frames and bare steel deck roof diaphragms.

Today in the U.S. seismic design provisions ASCE 7-16 [3], two different design methodologies exist for the seismic design of diaphragms. Traditional diaphragm design procedures assume the diaphragm demands are reduced by the response modification factor, R ($R_d R_o$ in Canada), which is associated with the vertical system alone. While, in the new alternative diaphragm design procedures, currently only applicable to concrete and wood diaphragms, a diaphragm response modification factor, R_s , is employed to reduce (or increase) the diaphragm demands based on the ductility and overstrength of the diaphragm alone. Today, there is no agreed upon R_s factor for steel deck or steel deck with concrete fill diaphragms.

To investigate the impact of different diaphragm design procedures on the seismic demands of the steel deck roof systems, a computational study using three-dimensional (3D) building models was conducted to study the nonlinear diaphragm behavior and its interaction with the nonlinear vertical LFRS. This paper focuses on a study employing a one-story archetype building with Concentrically Braced Frames (CBF) for the vertical system. A companion paper explores the performance of BRB-braced frames [4]. The modeling scheme capitalizes on the computational efficiency of calibrated frame and truss elements to capture the realistic nonlinear behavior of both the bracing system and the diaphragms. Nonlinear static pushover analyses and response

history analyses using 44 ground motions scaled to two hazard levels are performed to study the behavior and seismic performance of the buildings.

CALIBRATION AND MODELING STRATEGIES

The two key nonlinear building components examined herein are the diaphragm and the concentric braces in the frames. These two elements are calibrated using existing data and then appropriately modified for use in an archetype building. Calibration and the modeling details for these two elements are provided in the following two sections.

Diaphragm modeling

A steel deck roof diaphragm is selected for the archetype building. Experimental results from cantilever diaphragm tests are used to simulate the hysteretic behavior of a bare steel deck roof. The cantilever diaphragm test database established by O’Brien et al [5] was utilized to select appropriate specimens. For a typical bare steel deck roof diaphragm specimen 33 by Martin [6] with 20-gage P3615 1.5 in. B-deck was found to have sufficient design strength to match the demand for the baseline archetype building (detailed below) roof diaphragm (herein denoted as SP1).

Subsequent multi-story building studies currently under development employ a floor diaphragm with steel deck and concrete fill. Test specimen 3/6.25-4-L-NF-DT was used from an ongoing testing program [7], which consisted of 3 in. deck, with lightweight concrete fill and 6.25 in. total thickness (herein denoted as SP2). Figure 2 shows the cantilever diaphragm test and a simple computational model using two diagonal nonlinear truss elements with unit cross-section areas. The Pinching4 material model in *OpenSees* [8] is used for the truss elements to simulate the hysteretic behavior and capture cyclic strength and stiffness degradation behavior of the diaphragms.

A multi-level optimization procedure with independent objective functions including cumulative strain energy, peak load, and degradation slopes is developed to calibrate the material parameters of the Pinching 4 material. Table 2 shows calibrated Pinching 4 material parameters including backbone stresses and strains and cyclic strength and stiffness degradation for the two selected diaphragm specimens. The dimensions of the archetype building diaphragm units do not directly coincide with those of the test specimens, therefore the strategy described in [9] is adopted to modify the backbone parameters so that the diaphragm shear strength per unit length is consistently represented. A comparison of the hysteretic response from the calibrated diaphragm simulation and that from the experiment is shown in Figure .

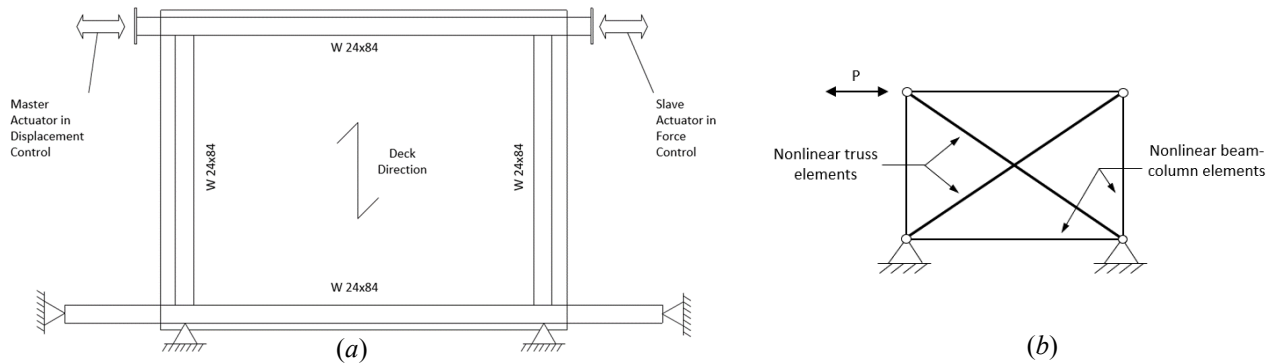


Figure 1. Cantilever diaphragm test: (a) schematic view of SP2 test setup, (b) computational model

Table 1. Calibrated Pinching4 Material Model Parameters

Test	Backbone		Pinching			Strength Degradation					Stiffness Degradation				Energy Dissipation			
	ϵ_1, σ_1 (MPa)	ϵ_2, σ_2 (MPa)	ϵ_3, σ_3 (MPa)	ϵ_4, σ_4 (MPa)	$r_{\Delta^+}, r_{\Delta^-}$	r_{p^+}, r_{p^-}	$u_{\Delta^+}, u_{\Delta^-}$	gF_1	gF_2	gF_3	gF_4	gF_{lim}	gK_1, gD_1	gK_2, gD_2	gK_3, gD_3	gK_4, gD_4	gK_{lim}, gD_{lim}	gE
SP1	0.0008, 152.9	0.0017, 199.2	0.0033, 211.6	0.0053, 165.3	0.20, 0.35	0.20, 0.35	0.10, 0.12	0	0.35	0	0.70	0.90	0, 0	0, 0.50	0, 0	0, 0.75	0, 0.90	4.31
SP2	0.0005, 437.6	0.0006, 526.8	0.0014, 740.5	0.014, 333.2	-0.06, -0.06	0.12, 0.12	0.11, 0.11	0	0.83	0.0	0.46	0.33	1.09, 0.14	0.76, 0.47	0.32, 0.12	0.75, 0.10	1.04, 0.61	4.29

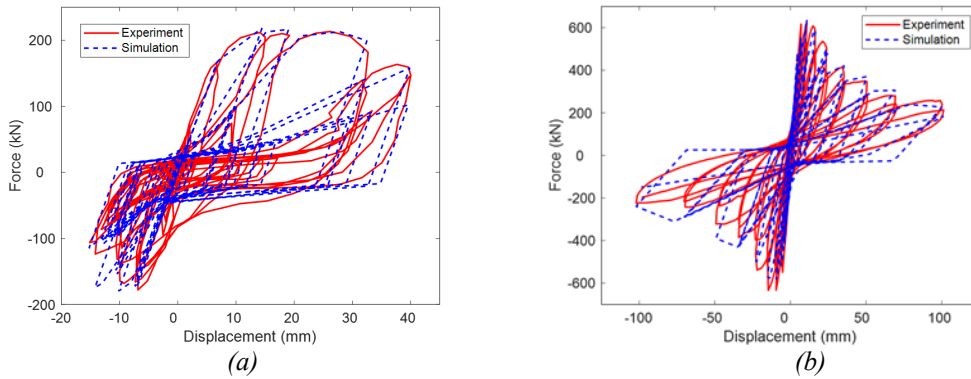


Figure 2. Hysteretic response of diaphragm from experiment and simulation: (a) SP1, (b) SP2

Brace modeling

Concentric braces are prone to buckle when they are under compression. To employ an accurate model to simulate the CBF behavior in both tension and compression, a computational *OpenSees* model is developed which is calibrated against experimental results. Experimental studies from Popov and Black [10], Fell et al. [11] and Han et al [12] (Figure 3a) are chosen to calibrate the computational model. The *OpenSees Steel02* material model as a fiber section is used to simulate the nonlinear behavior of a single brace under cyclic load. Figure 3b shows the detail of the concentric brace model. A hollow structural section with pinned boundary conditions is used in the computational model. Geometric imperfections equal to $L/1000$ is used in the middle of the brace, and the element is discretized into 10 elements along its length. Table 3 presents the *Steel02* material model parameters for three different studies. As can be seen in Figure 4, the model can capture the behavior of the brace in both tension and compression. It is important to note that this model of the brace neglects explicit modeling of local buckling and does not capture fracture in the braces or connections thus drift limits on the braced frames must be monitored.

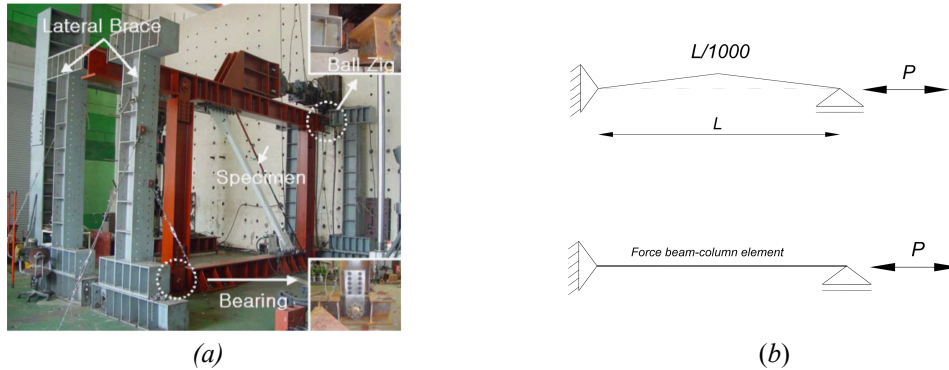


Figure 3. Detail of the concentric brace modelling: (a) Experimental test set up[10], (b) *OpenSees* model

Table 2. *Steel02* material model parameters for three different experimental studies

Experimental Study	F _y (Mpa)	b	R0	CR1	CR2	a1	a2	a3	a4
Popov and Black[9]	380	0.002	20	0.925	0.15	0	1	0.1	5
Fell et al.[10]	462	0.002	20	0.925	0.15	0	1	0.1	5
Han et al.[11]	414	0.002	20	0.925	0.15	0	1	0.1	5

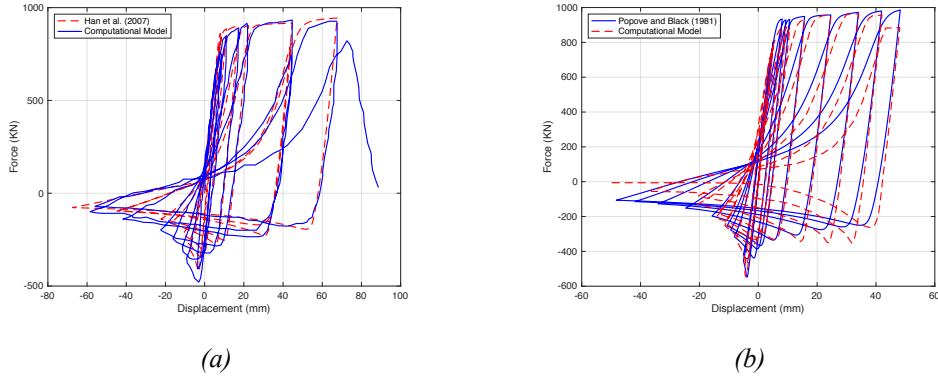


Figure 4. Hysteretic response of CBF from experiment and simulation: (a) Han et.al [10], (b) Popov and Black [9]

ARCHETYPE BUILDING

Archetype Design

For the current study, a one-story archetype building is designed and analyzed using the current U.S. seismic design provisions ASCE 7-16 and SAP2000 structural analysis software [11], respectively. Figure 5 shows the plan dimensions as 91.5 meters by 30.5 meters with a story height of 4.27 meters. The building has four bays braced with CBFs in each orthogonal direction. Bare steel deck was used at the roof under loads equal to 2.06 KN/m^2 dead and 0.96 KN/m^2 live load. The archetype buildings are assumed to be located in an arbitrary site in Irvine, California, with risk category II and site class D. The design spectral accelerations at short periods and at a 1-second period are 1.030g and 0.569g, respectively. More details of the archetype buildings can be found in [13].

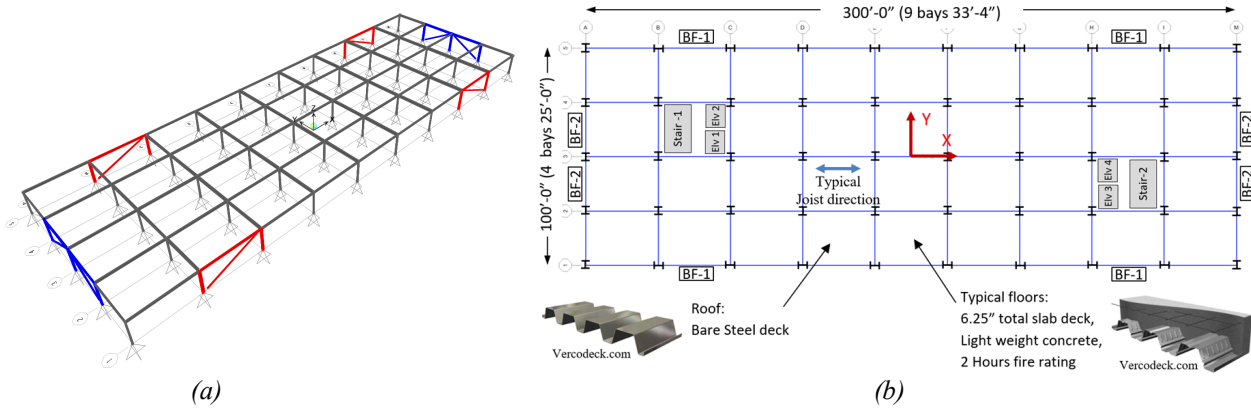


Figure 5. Schematic view of one-story archetype building: (a) 3D model, (b) typical plan

The diaphragm design force is 39.55 KN/m in the short direction of the building (weak direction of the diaphragm) for the one-story archetype building designed based on both traditional design forces in Section 12.10.1 of ASCE 7-16 and the alternative diaphragm design provisions ($R_s=3.0$). The first mode period from the design model is 0.36 s.

Archetype Simulation

A computational model of the archetype building was created in the software, *OpenSees*, with nonlinear elements for the diaphragm and concentric braces as previously described. All columns are pinned at their base. All beam-to-column and beam-to-beam joints are pinned with the exception of the braced bays which use semirigid connections at the beam-to-column joint to simulate the influences of the gusset plates. As recommended by FEMA P695 [14] the gravity loads include a combination of dead loads and live loads ($1.05D+0.25L$). Mass was determined from the dead loads and lumped at the column nodes on each floor. For nonlinear response history analysis, Rayleigh damping with a critical damping ratio equal to 2% for the 1st and 2nd mode is used for the archetype building models. Both material and geometric nonlinearity were considered in the analysis. Geometric nonlinearity was considered by including the gravity loads and using the P-Delta coordinate transformation algorithm in *OpenSees* for the columns. It is important to note that this model of the OCB neglects explicit modeling of local buckling and does not capture fracture in the braces or connections

ANALYSIS RESULTS

The 3D models of the archetype building were used to conduct several analyses. Eigenvalue analysis was performed to study the modal properties of the structures. Nonlinear static pushover analysis was performed to investigate overstrength, static ductility, and expected failure mode. Then, nonlinear response time history analyses were conducted over a suite of ground motions at different scale levels to evaluate the seismic performance and demand on the diaphragm in the archetype building.

EIGENVALUE ANALYSIS

The fundamental mode shapes and frequencies for the building model were calculated. The first mode is a sway mode in the short direction with a $T = 0.8s$. The difference between this OpenSees result and the SAP model is due to the flexibility of the diaphragm – the design model assumes a rigid diaphragm. These assumptions will be revisited in the future.

PUSHOVER ANALYSIS

Pushover analysis was conducted to study the static behavior of the archetype building. A displacement-controlled load pattern was applied to the structure in the short direction (long diaphragm span direction). Per FEMA P695, vertical distribution of the lateral force at each node was assigned proportional to the product of the tributary mass and the fundamental mode shape coordinate at the node obtained from eigenvalue analysis in *OpenSees*. Figure 6 shows the applied load versus the story drift for increasing values of drift ratios and the magnified displaced shape in the post-peak regime. The failure mode is dominated by loss of rigidity in the roof diaphragm.

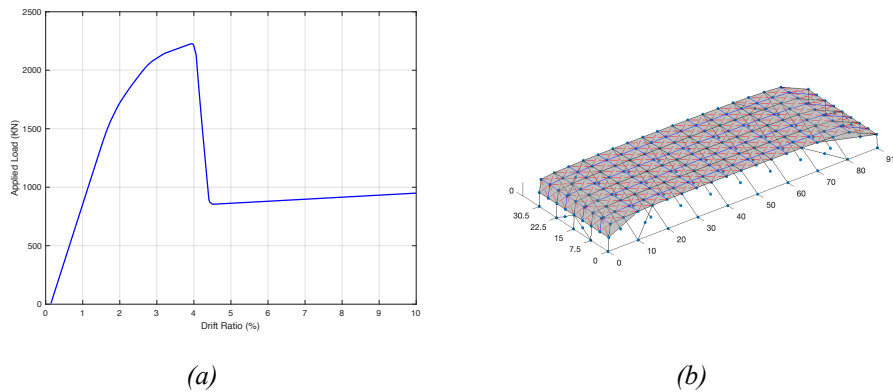


Figure 6. Pushover response of archetype building (a) force-displacement (b) post-peak displaced shape

To calculate the diaphragm ductility (μ), the post-peak displacement at 80% of the peak load is measured and divided by the yield displacement which is calculated using the displacement with the slope of 40% of the pre-peak load. The overstrength (Ω) of the diaphragm is calculated by dividing the peak load by the design base shear. Table 3 shows the values for the ductility and overstrength. The overstrength is relatively low as the braces are fully utilized, and the gravity frames are pinned, so essentially only the resistance factor against the brace buckling is providing overstrength in this case. The ductility is relatively low due to the large loss in strength after brace buckling. The residual force capacity in the model at large drift is presumably attributed to tensile membrane load paths in the roof, and must ultimately be drift limited due to fracture per discussions above.

Table 3. Ductility and overstrength of the building

Archetype	Design Shear (V_b) (KN)	Ductility (μ)	Overstrength (Ω)
One-story CBF	2226.7	1.61	1.11

NONLINEAR RESPONSE HISTORY ANALYSES

To evaluate the seismic performance of the archetype building and diaphragm system, nonlinear response time history analysis was performed with the building model subjected to the FEMA P695 suite of far-field earthquake motions. Two scale levels are considered for the nonlinear response history analysis: 1) Design basis earthquake (DBE) and 2) maximum considered earthquake (MCE). The 44 ground motions are scaled accordingly to each desired level and are applied in the weak direction of the building. For DBE and MCE, the ground motions are scaled such that the median spectrum matches the design spectrum at the fundamental period of the building. Based on the procedures, the scale factors for the two levels considered are 1.05 and 1.58, respectively.

The predicted diaphragm drift across the studied earthquakes is provided in Figure 7. The drift of the braced frames (perimeter story drift) and the drift (of the story) at the midspan of the diaphragm are primary quantities that are monitored. The midspan diaphragm drift is consistently greater than the perimeter story drift (Figure 7c-d and e-f) and peak diaphragm drifts are provided at the DBE and MCE level across all earthquakes in Figure 7a,b.

To provide an investigation of the detailed behavior the median earthquake, based on peak diaphragm drift demand, from the 44 analyzed is selected for detailed analysis. At the DBE level this is Earthquake 8 (1999 Hector Mine) in the P695 suite and at the MCE level this is Earthquake 34 (1987 Superstition Hills) in the P695 suite. Figure 7c-f provides the diaphragm drift and story drift at DBE and MCE levels for the median earthquake. As shown the peak of the diaphragm drift (midspan of the diaphragm) is almost twice that of the perimeter braced frame. Interestingly, the diaphragm also displays some higher frequency response than the braced frame. Note DBE median peak level diaphragm drift is 174 mm and MCE median peak diaphragm drift is 192 mm, even though the scale factor is 1.5 times greater for the MCE level the median diaphragm displacement only increases 11%. However, as Figure 7a-b show several earthquake simulations experience greatly increased drift demands as the scale changes from DBE to MCE.

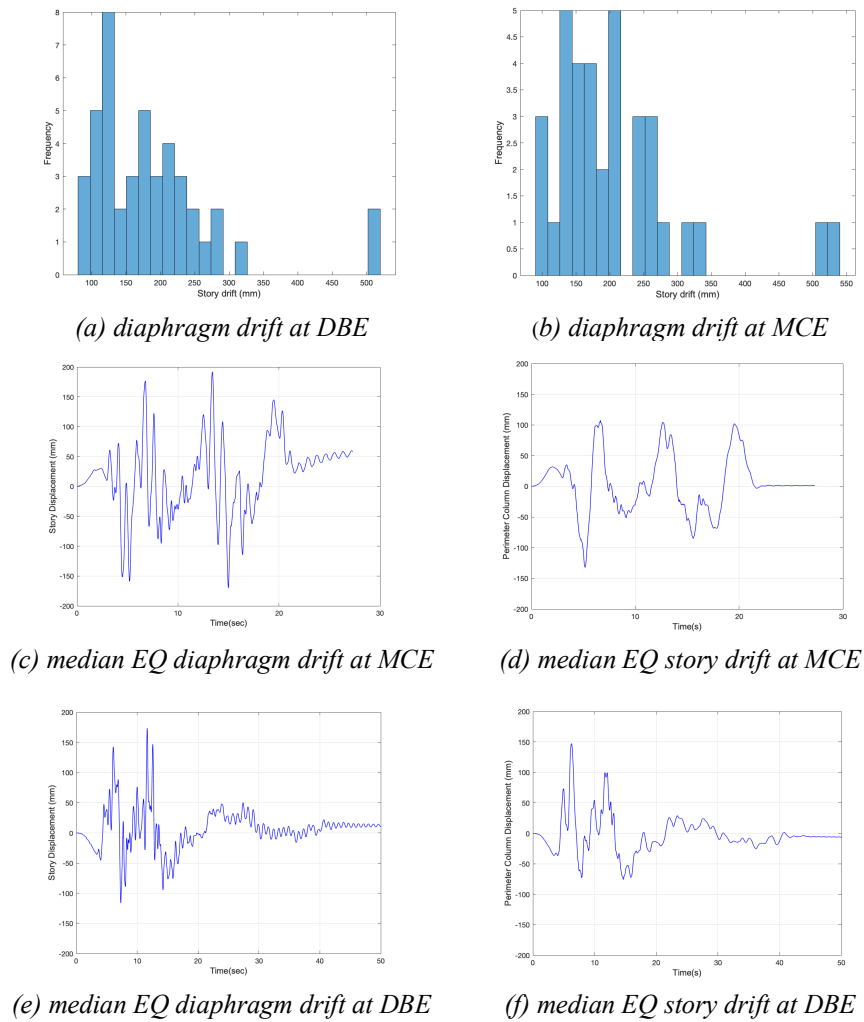


Figure 7. Measured building drifts across earthquake suite (a)-(b) and for median earthquakes (c)-(f)

Figure 8 provides time history of the base shear and the diaphragm force measured at the collectors on the short side of the building. At the MCE level the median base shear is 2283 kN vs. the design base shear of 2227 kN – indicating that the response is at or near the peak strength (see Figure 6). Note, the collectors take 1/2 of the base shear, as shown in Figure 8b.

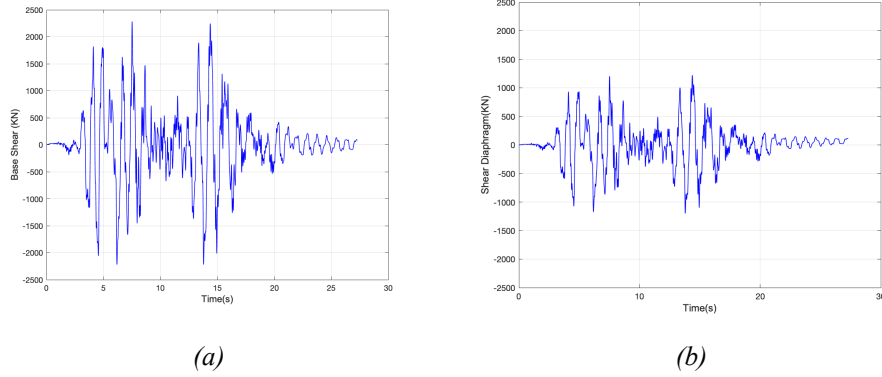


Figure 8. (a) Base shear of the archetype building (b) Diaphragm shear in collectors beam

Figure 9 provides the distribution of the diaphragm shear strain and the displaced shape of the model (top down) at the peak diaphragm drift from the median MCE-level earthquake. The results show that the peak roof shear strain in the diaphragm is about 0.5%. This may be compared with cyclically tested bare steel deck which has a peak shear strain of approximately 2% [5], indicating the median roof is not in a heavily damaged state in this model. Further indications of the lack of roof damage at this drift is the relatively smooth elastic displaced shape – as opposed to a more concentrated failure that occurs if the bare steel deck is damaged at its perimeter.

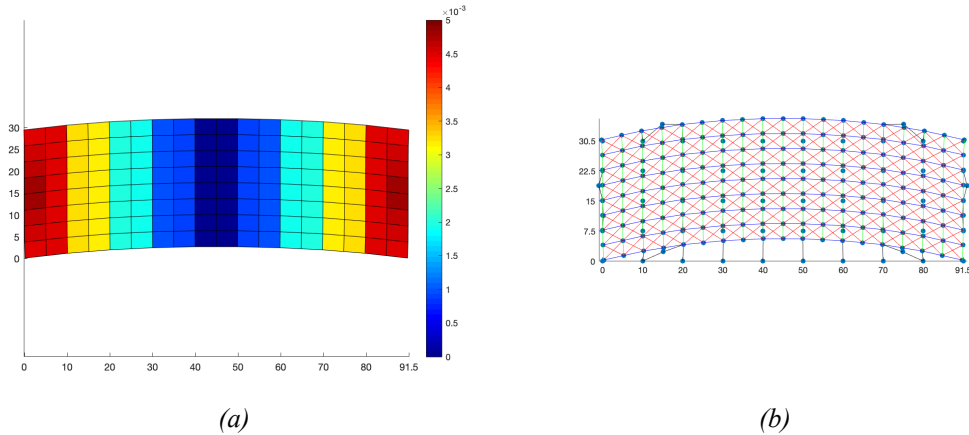


Figure 9. Roof response of median MCE scaled earthquake at peak diaphragm drift
(a) shear strain (b) displaced model, magnified 50X.

Figure 10 provides the axial force distribution in the perimeter beams (chords on the long side, collectors on the short side) of the archetype building at the time of peak diaphragm drift for the median MCE-level earthquake. As expected, the beams in the longer direction of the building are in tension in one side (red color) and in compression on the other side of the building (blue color). The distribution is influenced by the location of the braced bays, with larger axial forces in the braced bay to equilibrate the brace itself. The collector beams on the short side of the building have minimal axial force at the corners and maximum in the center, with the force in the beams dominated by the braces as opposed to the roof shear.

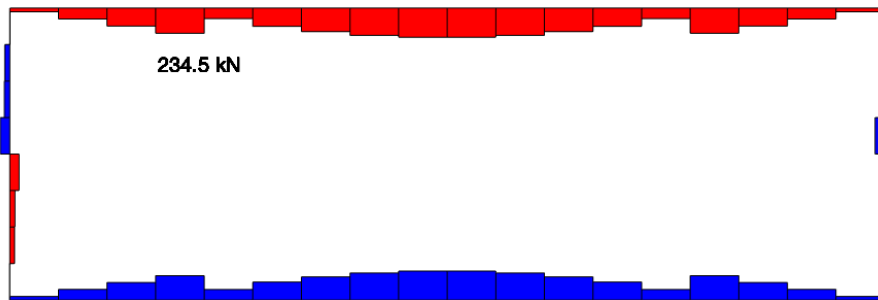


Figure 10. Axial force distribution in the perimeter beams of the archetype building median MCE earthquake at peak drift

Significant future work remains to provide definitive conclusions with this building archetype and further insights on the behavior of the diaphragm, chords, collectors, and concentric braced frames. In addition, parallel to the work in [4] a 4, 8, and 12-story archetype is currently under development. The impact of the CBF failure on the diaphragm demands is of primary interest for further studies. In addition, the impact of different diaphragm design methods on the frame, diaphragm, and overall building response in these archetypes is of interest. Though significant work remains, the models indicate that 3D building archetype studies can provide new insights on the seismic behavior of diaphragms in steel framed buildings.

CONCLUSIONS

As a first step in a larger study the seismic behavior of a single-story steel braced frame archetype building is studied herein. The building is designed using traditional U.S. seismic design provisions. A three-dimensional OpenSees model of the building is constructed. The model includes fiber sections for the braces calibrated to cyclic tests on hollow section concentric braces. The model also includes nonlinear truss elements for the in-plane shear behavior of the roof diaphragm calibrated to cyclic cantilever testing on bare steel deck diaphragms. The analysis indicates that the building has minimal overstrength and ductility, and its first limit state is related to brace buckling. At MCE levels, across the FEMA P695 earthquake suite, the median perimeter story drift is acceptable and the diaphragm response is essentially elastic. Examination of the diaphragm shear strains and the chord and collector forces indicates the diaphragm is behaving largely in accordance with the classical beam analogy at the studied demand level. Additional studies are planned and are currently underway.

ACKNOWLEDGMENTS

This work was supported by the National Science Foundation under Grant No. 1562669 and the Steel Diaphragm Innovation Initiative which is funded by AISC, AISI, SDI, SJI, and MBMA. Any opinions expressed in this paper are those of the authors alone, and do not necessarily reflect the views of the National Science Foundation.

REFERENCES

- [1] Rodriguez, M., Restrepo, J., and Blandón, J. (2007). Seismic design forces for rigid floor diaphragms in precast concrete building structures. *Journal of Structural Engineering*, 133(11), pp. 1604–1615.
- [2] EERI (1996). Northridge Earthquake Reconnaissance Report, Vol. 2 Earthquake Spectra - Supplement C to Volume 11 Earthquake Engineering Research Institute.
- [3] American Society of Civil Engineers. (2010). Minimum design loads for buildings and other structures (ASCE standard). Reston, Va.: American Society of Civil Engineers.
- [4] Wei, G., Foughi, H., Torabian, S., Schafer, B. W., and Eatherton, M. R. (2019). Evaluating Different Diaphragm Design Procedures Using Nonlinear 3D Computational Models. *12th Canadian conference on earthquake engineering*, Quebec, Canada.
- [5] O'Brien, P., Eatherton, M. R., & Easterling, W. S. (2017). Characterizing the load-deformation behavior of steel deck diaphragms using past test data.
- [6] Martin, É. (2002). Inelastic response of steel roof deck diaphragms under simulated dynamically applied seismic loading. Master's thesis, Ecole Polytechnique de Montreal.
- [7] Lowes, L. N., & Altoontash, A. (2003). Modeling reinforced-concrete beam-column joints subjected to cyclic loading. *Journal of Structural Engineering*, 129(12), 1686-1697.
- [8] Fillipou, F. C., Popov, E. P., & Bertero, V. V. (1983). Effect of bond deterioration on hysteretic behaviour of reinforced concrete joints. Report EERC 83-19. *Earthquake Engineering Research Center, University of California, Berkeley, Calif.*
- [9] Qayyum, B. (2017). Computational modeling of one-story buildings with nonlinear steel deck diaphragms subjected to earthquakes. Report, Virginia Tech.
- [10] Popov, E. P., and Black, R. G. (1981). Steel struts under severe cyclic loadings. *Journal of the Structural Division*, 107(9), pp. 1857-1881.
- [11] Fell, B.V., Kanvinde, A.M., Deierlein, G.G. and Myers, A.T., 2009. Experimental investigation of inelastic cyclic buckling and fracture of steel braces. *Journal of structural engineering*, 135(1), pp.19-32.
- [12] Han, S.W., Kim, W.T. and Foutch, D.A., 2007. Seismic behavior of HSS bracing members according to width–thickness ratio under symmetric cyclic loading. *Journal of Structural Engineering*, 133(2), pp.264-273.
- [13] Torabian, S., Eatherton, M.R., Easterling, W.S., Hajjar, J.F., Schafer, B.W. (2017) “SDII Building Archetype Design v1.0” CFSRC Report R-2017-04, permanent link: jhir.library.jhu.edu/handle/1774.2/40638.
- [14] Applied Technology Council. (2009). *Quantification of building seismic performance factors*. US Department of Homeland Security, FEMA.